

# Calibration of the maximum carboxylation velocity ( $V_{c_{max}}$ ) using data mining techniques and ecophysiological data from the Brazilian semiarid region, for use in Dynamic Global Vegetation Models

L. F. C. Rezende<sup>a\*</sup>, B. C. Arenque-Musa<sup>b</sup>, M. S. B. Moura<sup>c</sup>, S. T. Aidar<sup>d</sup>, C. Von Randow<sup>a</sup>,  
R. S. C. Menezes<sup>e</sup> and J. P. B. H. Ometto<sup>a</sup>

<sup>a</sup>Earth System Science Center, National Institute for Space Research - INPE, Av. dos Astronautas, 1758,  
Jd. Da Granja, CEP 12227-010, São José dos Campos, SP, Brazil

<sup>b</sup>Laboratory of Plant Physiological Ecology – LAFIECO, Department of Botany, Universidade de São Paulo – USP,  
Rua do Matão, 277, Cidade Universitária, CEP 05508-090, São Paulo, SP, Brazil

<sup>c</sup>Department of Agrometeorology, Embrapa Tropical Semiarid, Empresa Brasileira de Pesquisa Agropecuária –  
EMBRAPA, Rodovia BR-428, Km 152, Zona Rural, CEP 56302-970, Petrolina, PE, Brazil

<sup>d</sup>Department of Plant Ecophysiology, Embrapa Tropical Semiarid, Empresa Brasileira de Pesquisa Agropecuária –  
EMBRAPA, Rodovia BR-428, Km 152, Zona Rural, CEP 56302-970, Petrolina, PE, Brazil

<sup>e</sup>Department of Nuclear Energy, Universidade Federal de Pernambuco – UFPE,  
Av. Prof. Luis Freire, 1000, CEP 50740-540, Cidade Universitária, Recife, PE, Brazil

\*e-mail: luiz.rezende@inpe.br

Received: August 4, 2014 – Accepted: March 24, 2015 – Distributed: May 31, 2016  
(With 6 figures)

## Abstract

The semiarid region of northeastern Brazil, the *Caatinga*, is extremely important due to its biodiversity and endemism. Measurements of plant physiology are crucial to the calibration of Dynamic Global Vegetation Models (DGVMs) that are currently used to simulate the responses of vegetation in face of global changes. In a field work realized in an area of preserved *Caatinga* forest located in Petrolina, Pernambuco, measurements of carbon assimilation (in response to light and CO<sub>2</sub>) were performed on 11 individuals of *Poincianella microphylla*, a native species that is abundant in this region. These data were used to calibrate the maximum carboxylation velocity ( $V_{c_{max}}$ ) used in the INLAND model. The calibration techniques used were Multiple Linear Regression (MLR), and data mining techniques as the Classification And Regression Tree (CART) and K-MEANS. The results were compared to the UNCALIBRATED model. It was found that simulated Gross Primary Productivity (GPP) reached 72% of observed GPP when using the calibrated  $V_{c_{max}}$  values, whereas the UNCALIBRATED approach accounted for 42% of observed GPP. Thus, this work shows the benefits of calibrating DGVMs using field ecophysiological measurements, especially in areas where field data is scarce or non-existent, such as in the *Caatinga*.

**Keywords:** Dynamic Global Vegetation Models (DGVM), maximum carboxylation velocity ( $V_{c_{max}}$ ), *Caatinga*, Gross Primary Productivity (GPP), global changes.

## Calibração da velocidade máxima de carboxilação ( $V_{c_{max}}$ ), utilizando técnicas de mineração de dados e dados de ecofisiologia da região semiárida brasileira, para uso em Modelos de Vegetação Globais Dinâmicos.

## Resumo

A região semiárida do nordeste do Brasil, a *Caatinga*, é extremamente importante devido à sua biodiversidade e endemismo. Medidas de fisiologia vegetal são cruciais para a calibração de Modelos de Vegetação Globais Dinâmicos (DGVMs) que são atualmente usados para simular as respostas da vegetação diante das mudanças globais. Em um trabalho de campo realizado em uma área de floresta preservada na *Caatinga* localizada em Petrolina, Pernambuco, medidas de assimilação de carbono (em resposta à luz e ao CO<sub>2</sub>) foram realizadas em 11 indivíduos de *Poincianella microphylla*, uma espécie nativa que é abundante nesta região. Estes dados foram utilizados para calibrar a velocidade máxima de carboxilação ( $V_{c_{max}}$ ) usada no modelo INLAND. As técnicas de calibração utilizadas foram Regressão Linear Múltipla (MLR) e técnicas de mineração de dados como *Classification And Regression Tree* (CART) e K-MEANS. Os resultados foram comparados com o modelo INLAND não calibrado. Verificou-se que a Produtividade Primária Bruta (PPB) simulada atingiu 72% da PPB observada ao usar os valores de  $V_{c_{max}}$  calibrado, enquanto que o modelo

não calibrado obteve-se 42% da PPB observada. Assim, este trabalho mostra os benefícios de calibrar DGVMs usando medidas ecofisiológicas de campo, especialmente em áreas onde os dados de campo são escassos ou inexistentes, como na *Caatinga*.

**Palavras chave:** Modelos de Vegetação Globais Dinâmicos (DGVMs), velocidade máxima de carboxilação ( $V_{c_{max}}$ ), *Caatinga*, Produtividade Primária Bruta (PPB), mudanças globais.

## 1. Introduction

The semiarid region in Northeastern Brazil covers 844,453 km<sup>2</sup> (Brasil, 2014) and it is one of the most populated in the world and also concentrates the poorest population of the country (Brasil, 2010). A great portion of the population living in this region relies on agro pastoral activities and natural resources for subsistence. These activities are highly dependent on rainfall, and suffer setbacks due to adverse weather and recurrent drought cycles. Due to the scarcity of water, much of the soil presents low fertility, particularly regarding the levels of nitrogen, phosphorus and calcium. Currently, more than 10% of the semiarid area has suffered a very high degree of environmental degradation, being susceptible to desertification (Oyama and Nobre, 2004; Cunha et al., 2013; Santos et al., 2014). According to Sampaio et al. (2005), the area susceptible to desertification is reasonably defined, with a rate of precipitation by evapotranspiration less than 0.65. The *Caatinga* is an exclusively Brazilian biome and is extremely important due to a high biological diversity and the presence of many endemic species (Brasil, 2010). The *Caatinga* is a relatively poorly studied biome, compared to the other Brazilian biomes, despite the fact that it covers nearly 11% of the Brazilian territory. In 2012 and 2013 this region experienced one of the most severe drought events in 50 years (Santos et al., 2014). Dynamic Global Vegetation Models (DGVMs) are important tools for projecting environmental risks (potential consequences of climate change) and fostering discussions about a more sustainable future of the planet, or in this case of the *Caatinga* biome. However, models need calibration in order to be able to provide reliable answers. These models have a high sensitivity to parameters related to photosynthesis (Lebauer et al., 2013; Dietze, 2014).

The carboxylation velocity parameter ( $V_{c_{max}}$ ) is considered one of the most critical for changes in vegetation in face of global changes. The  $V_{c_{max}}$  is the measurement of process by which Rubisco catalyzes RuBP with CO<sub>2</sub> to produce the carbon compounds that eventually become triose phosphates (eg glyceraldeide-3P). Triose phosphates are the building block for sugars and starches.  $V_{c_{max}}$  has a direct impact on Gross Primary Productivity (GPP) (Bonan et al., 2012; LeBauer et al., 2013; Rogers, 2014; Dietze, 2014). Several uncertainties have been observed in the results of DGVM simulations and they tend to underestimate maximum GPP (Bonan et al., 2012; Dietze, 2014). This can be attributed to the lack of databases used for proper  $V_{c_{max}}$  calibration and the fact that canopy level  $V_{c_{max}}$  values are used, which are lower than those observed

at the leaf level (Schaefer et al., 2012; Dietze, 2014). Rogers (2014) noted a wide variation in  $V_{c_{max}}$  used in models that had identical PFTs (Plant Functional Types) and they sought to represent the CO<sub>2</sub> uptake of the same biomes, which is critical due to the role of  $V_{c_{max}}$  in the carbon cycle. The use of static parameters implies that DGVMs cannot adjust to environmental changes (Smith and Dukes, 2012). Physiological processes are considered the main sources of uncertainties in these models. However, it is expected that a plant physiology database will enable the calibration and correction of the models and thus reduce substantially these uncertainties in the next generation of DGVMs (LeBauer et al., 2013; Huntingford et al., 2013; Rogers, 2014; Dietze, 2014).

In this work, the objective is to calibrate the value of  $V_{c_{max}}$  used in the INLAND model (Tourigny, 2014) for the *Caatinga* biome using carbon assimilation (CO<sub>2</sub> curves) from field measurements. INLAND is derived from IBIS (Foley et al., 1996; Kucharik et al., 2000). We used the Multiple Linear Regression (MLR) technique for fitting  $V_{c_{max}}$  and the Classification And Regression Tree (CART) and K-MEANS algorithms to define classifications or groups of  $V_{c_{max}}$  values. The results of simulations of the INLAND model using the calibrated  $V_{c_{max}}$  values were compared to simulations using an uncalibrated configuration of the model. The goal of this work was to evaluate if the use of  $V_{c_{max}}$  measurements for model calibration would improve simulated GPP and NEE.

## 2. Material and Methods

### 2.1. Field work

The field work was conducted in a 600 ha area of preserved *Caatinga* forest, located in the headquarters of Embrapa Tropical Semiarid in Petrolina, Pernambuco, during the rainy seasons of February 2013 and 2014, with a purpose of performing CO<sub>2</sub> measurements. The *Caatinga* vegetation in this region Petrolina is classified as *Savannah Steppe trees and shrubs*. This type of *Caatinga* vegetation represents 75.72% of the total area of the *Caatinga* biome (Brasil, 2007). The soil of the experimental area is classified as Argisol, which is characterized by low water retention and poor fertility. *Caatinga* is characterized by low annual precipitation and prolonged drought periods (6-8 months each year). The rainy season in Petrolina is from December to April and the dry season is from May to October. In a data series from CPTEC-INPE covering 14 years (1997-2011), the monthly mean maximum temperatures reach their highest in November (~ 34°C) and the average monthly minimum temperatures reach

their lowest values in July (~20°C). The average monthly rainfall for this period shows that February is the month of highest rainfall (~88 mm); and August is the month of lowest rainfall (~1 mm). The *Poincianella microphylla* species (vulgar name: catingueira falsa) was selected because it has a high occurrence in the *Caatinga* and it belongs to the Fabaceae family, which represents 50.63% of the species in the area (Drummond et al., 2002). Following a direction (125° transect) and a distance of ~120 m from a meteorological tower (9° 2' 47.4144" S, 40° 19' 16.7154" W, altitude: 364.7), 11 individuals of *catingueira* were selected and geo-referenced using a Global Positioning System (GPS). This direction was selected following a prior study of the tower footprint, as part of *Caatinga* Flux Project. The heights of these individuals varied from 1.7 to 4.5 m. Physiological measurements were carried using a photosynthesis and fluorescence analyzer LI-6400 (Li-Cor, Nebraska, USA) and were performed on fully expanded and sun-exposed leaves (one leaf per plant), directly on the standing plants. Temperature of leaves and relative humidity of chamber were not controlled and they varied according to the environmental conditions. The time of measurements was between 7:00 (am) and 3:00 (pm) local time. In light response curves ( $A \times$  Photosynthetic Active Radiation – PAR) the points were: 800, 600, 400, 200, 100, 50, 25 and 0  $\mu\text{mol m}^{-2} \text{s}^{-1}$  performed under Light Emitting Diode (LED) source light with blue = 10% and  $\text{CO}_2$  flux fixed in 400  $\mu\text{mol mol}^{-1}$ . Some tests were performed for  $A \times$  PAR curves and we concluded that plants saturate in points close to 800  $\mu\text{mol m}^{-2} \text{s}^{-1}$  (instead 1500  $\mu\text{mol m}^{-2} \text{s}^{-1}$  that is the most common saturating light intensity for C3 species). We understand that even with a high amount of available light, water limitation makes this species have a more conservative strategy and not “cope well” with high radiation especially in times of the year where soil moisture is not abundant. The equations used to calculate the assimilation of  $\text{CO}_2$  ( $A$ ), stomatal conductance ( $g_s$ ) and intercellular concentration ( $C_i$ ) followed Von Caemmerer and Farquhar (1981). Applying model of non-rectangular hyperbola (Long and Hallgren, 1993)  $A \times$  PAR curves were performed in order to identify the plants' photosynthetic saturation point.

The curves of photosynthetic response to  $\text{CO}_2$  intercellular concentration ( $A \times C_i$ ) were performed under LED source light (red-blue, 10% blue) set to a PAR of 800  $\mu\text{mol photons m}^{-2} \text{s}^{-1}$ .  $\text{CO}_2$  curves were initiated with a  $\text{CO}_2$  air concentration of 400  $\mu\text{mol mol}^{-1}$  (e.g., 400 ppm) and decreased to 300, 200, 100, 50 until 0  $\mu\text{mol mol}^{-1}$ . In sequence, we injected increasing  $\text{CO}_2$  values of 400, 600, 900 and 1200  $\mu\text{mol mol}^{-1}$ . Carbon assimilation was estimated according to models of Farquhar et al. (1980), Von Caemmerer and Farquhar (1981), Farquhar and Von Caemmerer (1982), Von Caemmerer (2000) and it is expressed as a minimum of three main limitations in the plant capacity to fix carbon: light limited-rate of photosynthesis ( $A_j$ ), the limited rate Rubisco- for photosynthesis ( $A_c$ ) and the triose phosphate limitation in the using for photosynthesis ( $A_t$ ) (Equation 1):

$$A = \min (A_j, A_c, A_t) \quad (1)$$

It was not considered the triose phosphate limitation, thus  $A_c$  and  $A_j$  are estimated by Equations 2 and 3:

$$A_c = ([V_{c_{max}} (C_i - \Gamma^*)] / [C_i + K_c (1 + O/K_o)]) - R_d \quad (2)$$

Where  $V_{c_{max}}$  is maximum velocity of carboxylation;  $C_i$  is concentration intercellular;  $\Gamma^*$  is compensation point of  $\text{CO}_2$ ;  $K_c$  is the Michaelis-Menten constant for  $\text{CO}_2$ ;  $K_o$  is the Michaelis-Menten constant for  $\text{CO}_2$ ,  $O$  is partial pressure of  $\text{O}_2$  in equilibrium with its dissolved concentration in chloroplast stroma;  $R_d$  is mitochondrial respiration rate in the presence of light.

$$A_j = ([J_{max} (C_i - \Gamma^*)] / [4C_i + 8 \Gamma^*]) - R_d \quad (3)$$

Using the initial slope of the net assimilation rate in relation to  $C_i$  ( $C_i$  less than 200), it was calculated a maximum speed of Rubisco enzyme carboxylation ( $V_{c_{max}}$ ) for the results obtained from the limiting equation by the limited rate Rubisco ( $A_c$ ). The calculation of the maximum rate of electron transport ( $J_{max}$ ) was carried out by solving the equation that describes the points of  $A_j$ . The stomatal limitation was quantified by the method Farquhar and Sharkey (1982), described in details by Long and Bernacchi (2003).

## 2.2. Modeling work

The INLAND model uses 12 PFTs and the deciduous shrub PFT was used for the *Caatinga* region. Data are organized in a database (DB) (see Figure 1) and we used some environmental variables that have good (or reasonable) correlation (or anti-correlation) with photosynthesis, such as leaf-level Vapor Pressure Deficit (VpdL), air temperature ( $T_{air}$ ) and Photosynthetically Active Radiation (PARout) measured in the environment. Despite VpdL being used as an indicator of water availability, VpdL and soil water content are not always covariant (Beer et al., 2009). We use these variables to get a initial value of  $V_{c_{max}}$ , which is modified using a soil water stress factor, following the INLAND model (Equation 4):

$$V_{c_{max}} = Vc \times \text{stresstl} \quad (4)$$

where  $Vc$  is the  $V_{c_{max}}$  value obtained from learning machine (data mining) methods, MLR or UNCALIBRATED defined in INLAND for deciduous shrubs;  $\text{stresstl}$  is a value calculated by INLAND model from precipitation, radiation and air temperature data (collected in the meteorological tower) and it varies from 0 to 1. Using the field samples, the inferences were done with MLR and with the CART and K-MEANS unsupervised clustering methods. After calibration using these methods, the rules of CART and K-MEANS and the MLR equations were implemented in the INLAND model.

### 2.2.1. CART

CART is a method to perform a classification through categorical or discretized variables regression with average values as output (Breiman et al., 1984). This method was selected because it allows to supply a discretized real

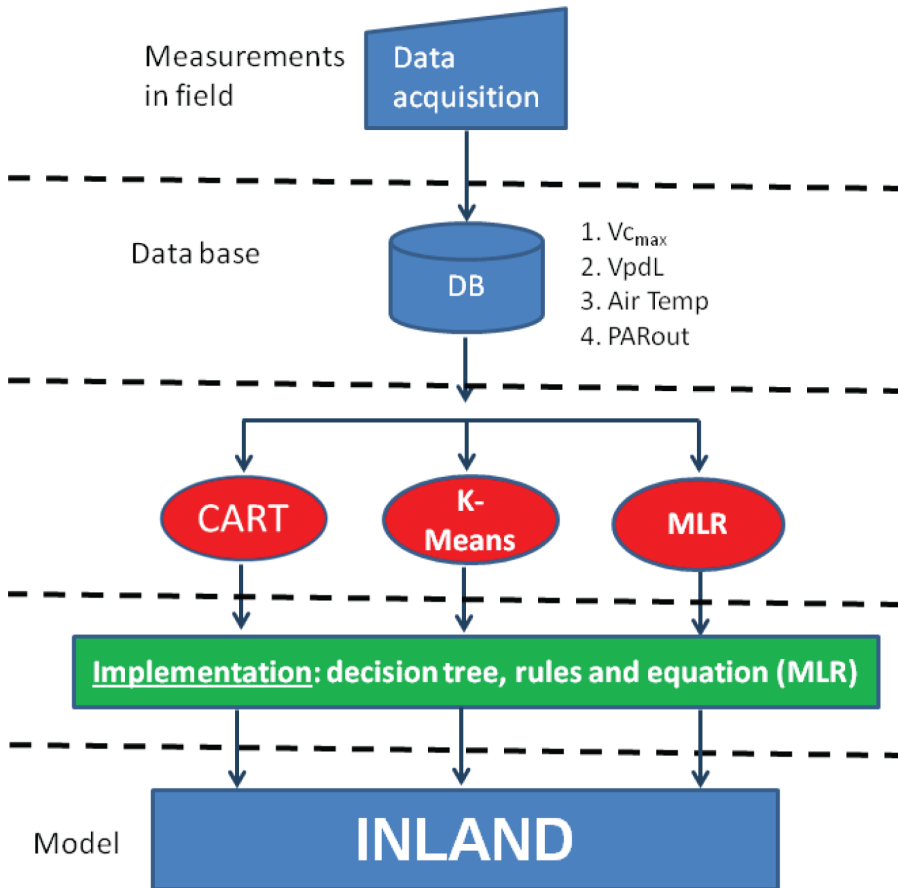


**Figure 1.** Illustration of the main parts of this work: data acquisition, database implementation, calibration (CART and K-MEANS machine learning approaches) and modeling.

variable (one value of  $V_{c_{max}}$ ) and it solves a multivariate regression problem. We used the CART implementation in Matlab software version 7.12. This method has other advantages such as the easiness to interpret the results; low sensitivity to outliers, ability to handle high dimensionality data (i.e. data with many attributes), and also to identify the more relevant parameters; requires little data preparation, whereas other techniques often need the normalization of data; as well as fast processing time and high accuracy (Sutton, 2005; Lima et al., 2014).

CART input is a set of chained rules such as "IF THEN ELSE", forming a hierarchical structure similar to a tree. It operates on a database and determines the output parameter class based on input attributes. The components of this structure basically are: nodes - rules that test the values (or attributes); leaves - the classification itself. Each path in the tree (from root to leaf) corresponds to a classification rule. The attribute space (in this case: VpdL, air temperature and PAR) were partitioned by binary splitting of the input attributes. Each splitting corresponds to a rule concerning the value of the output attribute, being depicted by a node of the tree. At each node, the left or right branch is chosen according to the

value of the considered input attribute, i.e. according to a simple less than (equal) or greater than (equal) rule (value comparison rule). In this fashion, at some terminal node a "final" discrete value is assigned to the output attribute. One of the criteria for choosing the attribute for a node is the choice of the attribute which has highest information gain that is realized through entropy estimate (more or less organized data) (Han and Kamber, 2001). A decision tree has many levels and the same attribute may appear many times in different nodes/levels. A pruning criteria is adopted in order to avoid overfitting, which renders a tree that is not able to perform classification/regression in a dataset different from the training set (Han and Kamber, 2001; Witten et al., 2011).

#### 2.2.2. K-MEANS (Clustering)

We used the K-MEANS implementation of Weka software version 3.7.1 released under the GNU General Public License. First the K parameter, which represents the number of groups or cluster to be classified, is determined. K points are chosen at random as cluster centroids by the algorithm. Instances are assigned to their closest cluster centroid according to a distance function (in our

case, we apply Euclidean distance). Next the centroid, or mean, of all instances in each cluster is calculated – this is the “means” part. These centroids are taken to be new center values for their respective clusters. Finally, the whole process is repeated with the new cluster centroids. Iteration continues until the same points are assigned to each cluster in consecutive rounds, at which point the cluster centroids have stabilized and will remain the same thereafter (Witten et al., 2011). The data were normalized in order to transform values between 0 and 1. The normalization purpose in this case is that magnitude of the attribute (for example: PARout) could have larger weight in the distance calculation.

### 2.2.3. Uncalibrated approach

We used the INLAND parameterization defined for  $V_{c_{max}}$  of deciduous shrubs PFTs as  $27.5 \times 10^{-6} \text{ mol m}^{-2} \text{ s}^{-1}$  at  $15^\circ\text{C}$  (Kucharik et al., 2000), which is uncalibrated for *Caatinga*.

### 2.2.4. Data input and data for comparison

Additional data sets were used: one as input forcing (meteorological data) and another as environmental variables for comparison between observed data and modeled data. Forcing data were incident short and long wave solar radiation (measured with Kipp & Zonen, Inc., pyranometers and pyrgeometers facing up and down at a height of 9 m from the ground), air temperature and relative humidity (measured with Vaisala, Inc., model HMP 45C-L probe at the same height as the radiation sensors), horizontal wind velocity (measured with R. M. Young Company Wind Sentry anemometers) and rainfall data (collected with a Hydrological Services, Pty Ltd., TB4 rain gauge). The measured data used for the estimation of GPP and NEE (as explained in the next section) were hourly time series of incoming and reflected photosynthetically active radiation (PAR), net radiation ( $R_n$ ), friction velocity ( $u$ ), sensible heat flux ( $H$ ), and latent heat flux ( $LE$ ). PAR was measured with a Kipp & Zonen PAR-Lite sensor.  $R_n$  was acquired with a Kipp&Zonen NR-Lite net radiometer at 10m above the ground.

### 2.2.5. Gap-filling of the eddy covariance and meteorological data

GPP and NEE were estimated through the Eddy Covariance gap-filling and flux-partitioning tool that is provided by the Max Planck Institute for Biogeochemistry (Reichstein et al., 2005; Max Planck Institute for Biogeochemistr, 2014). This method allows filling missing values in a time series. The gap-filling of the eddy covariance method also considers the co-variation of fluxes with meteorological variables and the temporal auto-correlation of the fluxes (Reichstein et al., 2005). In this algorithm, three different conditions are identified: 1) Only the data of direct interest are missing, but all meteorological data are available; 2) Additionally air temperature or VPD is missing, but radiation is available; 3) Radiation data is also missing. In the final comparison, missing values are not considered in the evaluation of the results (Reichstein et al., 2005).

## 3. Results

In this section we show results of field measurements, model calibration using these measurements and simulations using the calibration.

### 3.1. Ecophysiological measurements

$\text{CO}_2$  response and light response curves were measured in the field to estimate the vegetation responses in *caatingeira falsa* during two periods: February 4-8, 2013 and February, 23-27, 2014, both during the rainy season. Data shows a negative correlation between  $V_{c_{max}}$  and VpdL of  $-0.78$  for measurements of  $\text{CO}_2$  at  $400 \mu\text{mol mol}^{-1}$ .

In the 2014 campaign, four outlying values of  $V_{c_{max}}$  were higher than  $200 \mu\text{mol m}^{-2} \text{ s}^{-1}$  (203, 226.3, 226.4 and 211) and were discarded from statistical analysis. However only four points were discarded, we think it is important to register these values because there are few (or quasi no) data of  $V_{c_{max}}$  and  $\text{CO}_2$  curves for *Caatinga* for comparison (as shown in Table 1).

### 3.2. Model adjustment of $V_{c_{max}}$

In this section, we show the regression or calibration of  $V_{c_{max}}$  based on simulated values of GPP and NEE.

#### 3.2.1. Calibration with Multiple Linear Regression (MLR)

Using MLR we obtained the following fitting Equation 5:

$$V_{c_{max}} = -109.7 - 38.3 \text{ VpdL} + 9.75 \text{ TempAir} - 0.03 \text{ PARout} \quad (5)$$

It shows that the attribute of highest weight in the linear regression was VpdL with  $-38.3$ ; air temperature was second in significance with  $9.75$  and PARout was very small:  $0.03$ . It has reasonable correlation:  $0.57$  and root mean squared error of  $38.0$  (see Figure 2).

#### 3.2.2. Calibration with CART

The CART decision tree learning technique was used to map the value of  $V_{c_{max}}$  based on rules related to observed VpdL and air temperature. The inferred rules are illustrated in Figure 3, where each triangle represents a decision level. For example, in the first level (the top triangle), we can see following decision: – if VpdL is equal or greater than  $3.3$ ,  $V_{c_{max}}$  is classified as  $47.0 \mu\text{mol CO}_2 \text{ m}^{-2} \text{ s}^{-1}$ . Each filled circle is a terminal node, the end of a branch in the

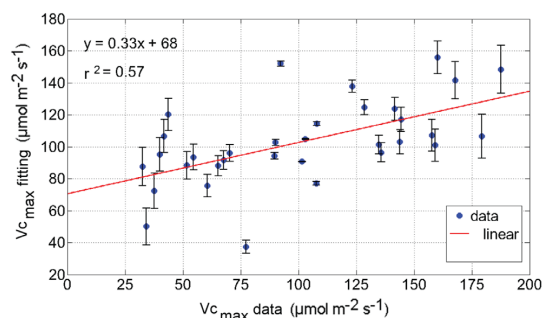


**Figure 2.** Dispersion of MLR for  $V_{c_{max}}$  and bar of standard error of mean – ( $n=33$ ).

**Table 1.** Results of  $Vc_{max}$  estimated through field data and its standard errors of the means (SEM) (n=37).

VpdL (kPa)	±	Temp.Air (°C)	±	PARout ( $\mu\text{mol photons m}^{-2} \text{s}^{-1}$ )	±	$Vc_{max}$ ( $\mu\text{mol m}^{-2} \text{s}^{-1}$ )	±	Vcmax (at 25°C) ( $\mu\text{mol m}^{-2} \text{s}^{-1}$ )	±
4.49720	0.34	38.5	0.80	701.6	8.3	37.7	12.4	13.0	7.5
4.43847	0.33	38.4	0.78	1914.4	207.7	77.3	5.9	26.5	5.3
4.02850	0.26	37.8	0.68	963	51.3	60.6	8.7	22.4	6.0
3.27095	0.13	35	0.22	179.5	77.4	159.1	7.4	71.5	2.0
3.46174	0.16	34	0.06	1304	107.4	34.2	13.0	14.6	7.3
2.30124	0.02	31.6	0.33	652.9	0.3	101.5	1.9	60.1	0.1
1.96733	0.07	30	0.59	647.3	0.5	65.3	7.9	44.2	2.4
2.35285	0.01	32	0.26	524.2	20.7	135.8	3.6	77.1	2.9
3.44329	0.16	35.8	0.35	408.7	39.7	40	12.0	16.9	6.9
3.21498	0.12	35.2	0.26	243.3	66.9	143.9	4.9	64.7	0.9
1.24668	0.19	32.4	0.19	184.9	76.5	226.3	18.5	123.2	10.5
1.21799	0.19	33	0.10	316.6	54.8	160.2	7.6	83.3	3.9
1.09090	0.21	32	0.26	632.7	2.9	167.8	8.9	98.5	6.4
1.40622	0.16	32.6	0.16	197.6	74.4	187.6	12.1	101.2	6.9
1.79958	0.10	35.1	0.24	854.7	33.5	226.4	18.5	96.1	6.0
2.64427	0.03	38.5	0.80	1923.3	209.2	41.9	11.7	14.3	7.3
2.42536	0.00	37	0.55	1533.7	145.1	203.1	14.7	72.9	2.2
3.20736	0.12	38.3	0.77	796.5	23.9	144.4	5.0	46.9	2.0
3.38247	0.15	39.3	0.93	1877.2	201.6	32.5	13.3	10.7	6.0
2.97034	0.08	37.1	0.57	484.7	27.2	141.7	4.6	54.9	0.6
2.97897	0.09	35.9	0.37	201.2	73.8	43.7	11.4	17.3	6.8
3.17688	0.12	36.3	0.44	532.9	19.3	179.3	10.8	70.1	1.8
1.17687	0.20	28.3	0.87	220.1	70.7	107.9	0.9	83.8	7.9
1.38237	0.17	31.6	0.33	254.5	65.1	123.2	1.5	75.4	2.6
1.76653	0.10	34.1	0.08	1014.6	59.8	128.5	2.4	59.2	0.0
2.44282	0.00	37.6	0.65	1871.3	200.6	157.7	7.6	60.2	0.1
1.92229	0.08	27.3	1.03	188.5	75.9	107.7	0.9	85.8	4.3
2.05905	0.06	29.1	0.74	227	69.6	51.8	10.1	37.6	3.5
1.83197	0.09	28.8	0.79	222.9	70.3	89.6	3.9	68.4	1.5
1.85148	0.09	28.5	0.84	187.5	76.1	67.6	7.5	52.1	1.1
1.87569	0.09	29.8	0.62	211.3	72.2	90.1	3.8	65.9	1.1
1.89957	0.08	35.2	0.26	291.2	59.0	92.3	3.4	63.1	0.3
2.07286	0.05	30.8	0.46	506.2	23.7	70.3	7.1	44.9	2.3
2.05267	0.06	30.6	0.49	291.6	59.0	134.8	3.4	84.6	4.1
2.20861	0.03	31.6	0.33	556.5	15.4	211	16.0	119.7	9.9
2.32679	0.01	31.4	0.36	460.2	31.2	54.6	9.6	31.4	4.5
2.44251	0.00	33.1	0.08	491.6	26.1	103	1.7	55.6	0.5

classification. Otherwise, if VpdL is less than 3.3, the process flows to next decision level (triangle).

After implementing the rules derived from the CART tree in INLAND, we can see (as shown in Table 2) that node 2 had a major occurrence (74.9%) of  $Vc_{max}$  of  $94.7 \mu\text{mol CO}_2 \text{ m}^{-2} \text{ s}^{-1}$  and node 4 had less occurrence (0.11%) for a  $Vc_{max}$  of  $159.7 \mu\text{mol CO}_2 \text{ m}^{-2} \text{ s}^{-1}$ . Two nodes (1 and 5) with  $Vc_{max}$  less than  $48 \mu\text{mol CO}_2 \text{ m}^{-2} \text{ s}^{-1}$  had

some significance (both summing 24.9%). Three nodes (3, 6 and 7) had no classified instances.

### 3.2.3. Calibration with K-MEANS

We choose five centroids/groups, which allows for a good distribution of discretized  $Vc_{max}$  (with a larger number of centroids the borders could be very close). Except for  $Vc_{max}$ , the attribute values used were normalized centroids

(between 0 and 1, as shown in Table 3). Thus these values are proportional to the highest sample of each attribute. We can see that in Group 4 there are high values of VpdL (0.7393) and air temperature (0.8312), characterizing a hot and dry environment, which is responsible for low  $V_{c_{max}}$  (45.9  $\mu\text{mol CO}_2 \text{ m}^{-2} \text{ s}^{-1}$ ). On the other hand, in Group 5 we can see a low VpdL (0.1524), an intermediate air temperature (0.4143) and high  $V_{c_{max}}$  (148.2  $\mu\text{mol CO}_2 \text{ m}^{-2} \text{ s}^{-1}$ ). We implemented the results and rules derived of Table 3 and the calculation of distances from instances to centroids in the INLAND model. Table 4 shows the results for each discretized  $V_{c_{max}}$  (the number of classified instances and percentage for each group). The group with highest number of classifications was Group 1, with 70.9% of total cases, and the group with less number of cases was Group 5, with 1.31% of total cases.

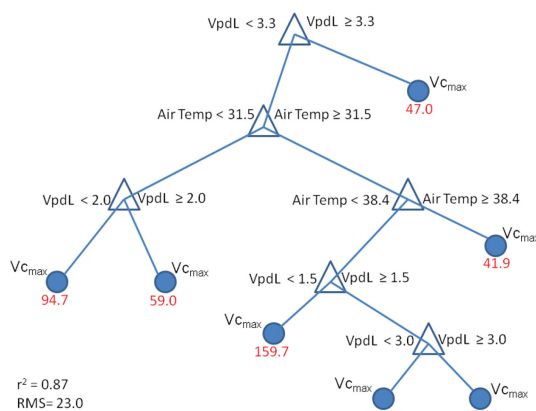


**Figure 3.**  $V_{c_{max}}$  ( $\mu\text{mol m}^{-2} \text{ s}^{-1}$ ) classification tree for the CART algorithm.

**Table 2.** Number and percentage of occurrences for each  $V_{c_{max}}$  node using the CART calibration.

	Node 1	Node 2	Node 3	Node 4	Node 5	Node 6	Node 7
Occurrences	4165	17361	0	27	1606	0	0
%	17.9	74.9	0	0.11	6.9	0	0
$V_{c_{max}}$	47.0	94.7	59.0	159.7	41.9	113.0	156.6

**Table 3.** Results of attribute centroids for the K-MEANS algorithm.

Attribute	Group 1	Group 2	Group 3	Group 4	Group 5
VpdL	0.1881	0.5743	0.3117	0.7393	0.1524
Temp. of air	0.1033	0.7736	0.3583	0.8312	0.4143
$V_{c_{max}}$	92.5	154.3	76.9	45.9	148.2

**Table 4.** Classification results of  $V_{c_{max}}$  using the K-MEANS algorithm.

	Group 1	Group 2	Group 3	Group 4	Group 5
Occurrences	18179	882	2478	3755	338
%	70.9	3.4	9.6	14.6	1.3
$V_{c_{max}}$	92.5	154.3	76.9	45.9	148.2

Both algorithms (CART and K-MEANS) had few cases with high  $V_{c_{max}}$  (greater than 154  $\mu\text{mol CO}_2 \text{ m}^{-2} \text{ s}^{-1}$ ) with 3.44% and 0.11% of total cases, respectively. The node with major number of occurrences (74.9%) with the CART algorithm was Node 2 with  $V_{c_{max}}$  of 94.7  $\mu\text{mol CO}_2 \text{ m}^{-2} \text{ s}^{-1}$ , whereas the group with a major number of occurrences (70.9%) using the K-MEANS method was Group 1 with a  $V_{c_{max}}$  of 92.5  $\mu\text{mol CO}_2 \text{ m}^{-2} \text{ s}^{-1}$ . These values are also closer to a simple mean value of  $V_{c_{max}}$  (101.01  $\mu\text{mol CO}_2 \text{ m}^{-2} \text{ s}^{-1}$ ) obtained from the 2013 and 2014 the campaigns, compared to others nodes and groups.

### 3.2.4. GPP

The CART, UNCALIBRATED, K-MEANS and MLR approaches reproduced the GPP variability in comparison with observed GPP (see Figure 4). However, the results for the UNCALIBRATED case were highly underestimated (around 6  $\mu\text{mol CO}_2 \text{ m}^{-2} \text{ s}^{-1}$  in the peak) when observed GPP was around 25  $\mu\text{mol CO}_2 \text{ m}^{-2} \text{ s}^{-1}$  in the rainy months (March-June) (Figure 4a-d). K-MEANS was very reasonable when the productivity was around 24  $\mu\text{mol CO}_2 \text{ m}^{-2} \text{ s}^{-1}$  in the month of May (Figure 4a-e). For the months of November and December, K-MEANS was very accurate and GPP reached two peaks with values of ~ 19  $\mu\text{mol CO}_2 \text{ m}^{-2} \text{ s}^{-1}$  and 23  $\mu\text{mol CO}_2 \text{ m}^{-2} \text{ s}^{-1}$  against observations of ~18  $\mu\text{mol CO}_2 \text{ m}^{-2} \text{ s}^{-1}$  and 24  $\mu\text{mol CO}_2 \text{ m}^{-2} \text{ s}^{-1}$ . Other approaches (CART and MLR) also had reasonable results for the peaks of November and December, but somewhat less accurate than K-MEANS. In these two months, CART had peaks of 18 and 19  $\mu\text{mol CO}_2 \text{ m}^{-2} \text{ s}^{-1}$  (Figure 4c); UNCALIBRATED two peaks of 10  $\mu\text{mol CO}_2 \text{ m}^{-2} \text{ s}^{-1}$  (Figure 4d); MLR 19 and 20  $\mu\text{mol CO}_2 \text{ m}^{-2} \text{ s}^{-1}$  (Figure 4f). All approaches showed reasonable results during the dry months. A few pulses of precipitation of 4 mm influenced the model between September and October, which allowed for peaks of productivity of 11, 10 and 13  $\mu\text{mol CO}_2 \text{ m}^{-2} \text{ s}^{-1}$ .

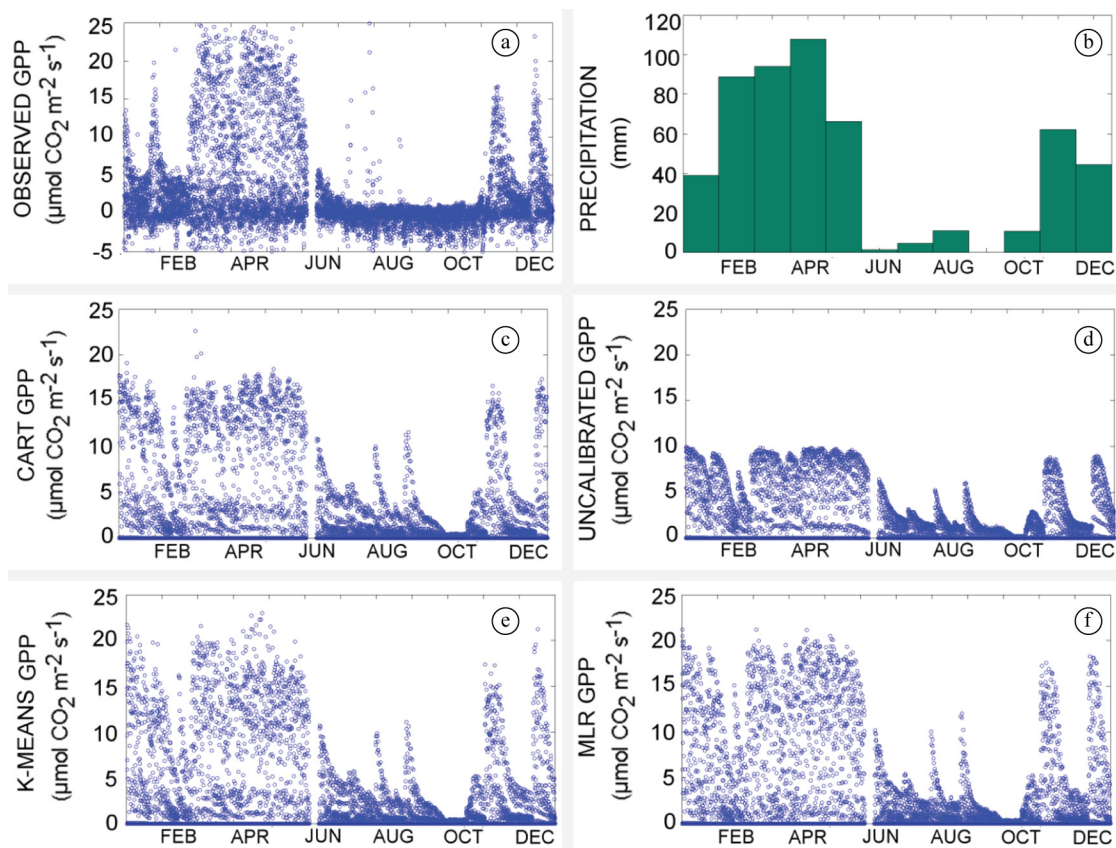


**Figure 4.** Data from 2011 - resolution of 1 hour: (a) Observed GPP; (b) Observed precipitation; (c) CART GPP; (d) UNCALIBRATED GPP; (e) K-MEANS GPP; (f) MLR GPP.

$\text{CO}_2 \text{ m}^{-2} \text{ s}^{-1}$  for CART; 8, 6 and 7  $\mu\text{mol CO}_2 \text{ m}^{-2} \text{ s}^{-1}$  for UNCALIBRATED; 11, 10 and 12  $\mu\text{mol CO}_2 \text{ m}^{-2} \text{ s}^{-1}$  for K-MEANS and 10, 11 and 14  $\mu\text{mol CO}_2 \text{ m}^{-2} \text{ s}^{-1}$  for MLR. All approaches showed high values of productivity between the months of January and February, when observed data show low productivity ( $\sim 5 \mu\text{mol CO}_2 \text{ m}^{-2} \text{ s}^{-1}$ ) with one peak of  $\sim 20 \mu\text{mol CO}_2 \text{ m}^{-2} \text{ s}^{-1}$ . The reason for this initially high productivity is that the **stress1** variable defined in Equation 4 is initialized to 1.0 in a situation of no water stress and evolves through time following changes in meteorological data such as precipitation and air temperature. None of the approaches produce negative values of GPP. The UNCALIBRATED approach reached low values of GPP. The  $V_{c_{\max}}$  value ( $27.5 \cdot 10^{-6} \text{ mol m}^{-2} \text{ s}^{-1}$  at  $15^\circ\text{C}$ ) used in this approach is low when compared to the values reached through the CART, K-MEANS and MLR approaches.

We calculated mean GPP during months March-May, which is during the rainy season (see Figure 4b), during which a major production is expected compared to other periods of this year (2011). Notable is the fact that GPP simulated with the MLR approach (mean of  $4.21 \mu\text{mol CO}_2 \text{ m}^{-2} \text{ s}^{-1}$ ) was closer to observed GPP ( $5.99 \mu\text{mol CO}_2 \text{ m}^{-2} \text{ s}^{-1}$ ) during this period. However results for the K-MEANS approach were nearest to observed GPP. The UNCALIBRATED approach

had the lowest values of  $V_{c_{\max}}$  and the production was underestimated with a mean value of  $2.54 \mu\text{mol CO}_2 \text{ m}^{-2} \text{ s}^{-1}$ .

In the analysis of bias and correlation of GPP, all approaches had a reasonable (good) correlation with observed GPP data: CART ( $r^2: 0.69$ ), UNCALIBRATED ( $r^2: 0.702$ ), K-MEANS ( $r^2: 0.703$ ) and MLR ( $r^2: 0.716$ ). The totals of GPP and NEE were calculated monthly (Figure 5). In Figure 5a, it was observed in the productivity peak (April, 2011) that 3 approaches (MLR, K-MEANS and CART) had values of GPP  $\sim 3100$ ,  $\sim 3000$  and  $\sim 3000 \mu\text{mol CO}_2 \text{ m}^{-2} \text{ s}^{-1}$ , respectively, when observed GPP was of  $\sim 4800 \mu\text{mol CO}_2 \text{ m}^{-2} \text{ s}^{-1}$ . However UNCALIBRATED simulated low productivity in comparison with observed GPP:  $\sim 2000 \mu\text{mol CO}_2 \text{ m}^{-2} \text{ s}^{-1}$ . In the months of July until October, observed GPP was negative, none of approaches reached the  $0 \mu\text{mol CO}_2 \text{ m}^{-2} \text{ s}^{-1}$  value. In the months of November and December, three approaches (CART, K-MEANS and MLR) agreed with observed data (productivity:  $\sim 1800 \mu\text{mol CO}_2 \text{ m}^{-2} \text{ s}^{-1}$ ). Again, UNCALIBRATED approach (productivity:  $\sim 1100 \mu\text{mol CO}_2 \text{ m}^{-2} \text{ s}^{-1}$ ) was lower than observed data. In the analysis of correlation of GPP monthly totals, all approaches had very good correlation with observed GPP data: CART ( $r^2: 0.93$ ), UNCALIBRATED ( $r^2: 0.93$ ), K-MEANS ( $r^2: 0.94$ ) and MLR ( $r^2: 0.94$ ).



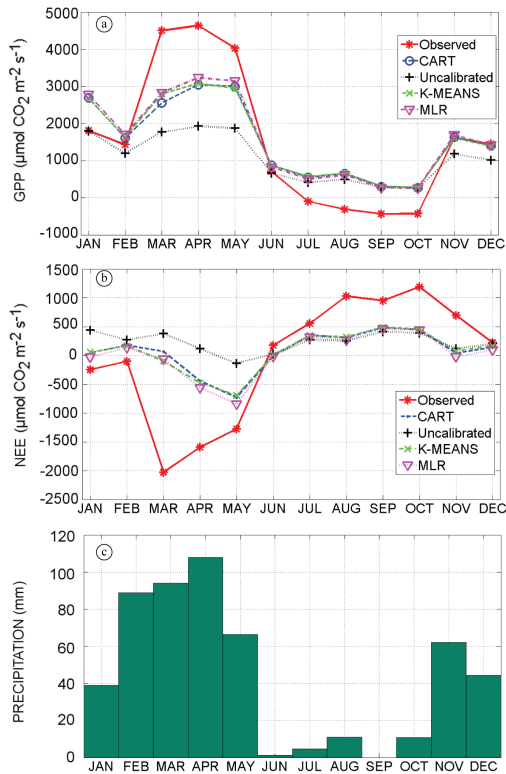


**Figure 5.** Monthly means – 2011: (a) GPP; (b) NEE; (c) Precipitation.

### 3.2.5 NEE

The CART, UNCALIBRATED, K-MEANS and MLR approaches reproduced the NEE variability compared to observed NEE (see Figure 6). However, all approaches showed a lower amplitude of NEE than observed. UNCALIBRATED results are more underestimated, with around  $-5 \mu\text{mol CO}_2 \text{ m}^{-2} \text{ s}^{-1}$  during the rainy period (March-June/2011), whereas observed NEE was around  $-20 \mu\text{mol CO}_2 \text{ m}^{-2} \text{ s}^{-1}$  (see Figure 6a-c). The K-MEANS approach show results closer to observed data when the negative amplitude was around  $-13 \mu\text{mol CO}_2 \text{ m}^{-2} \text{ s}^{-1}$  in May (see Figure 6a-f). CART, MLR and K-MEANS reproduce all seasonal variations associated to precipitation throughout the year and the mean difference is around  $-10 \mu\text{mol CO}_2 \text{ m}^{-2} \text{ s}^{-1}$  (Figure 6d-f). The difference is larger for UNCALIBRATED than for the other approaches ( $-15 \mu\text{mol CO}_2 \text{ m}^{-2} \text{ s}^{-1}$ ). All approaches reproduce the negative peaks in November and December (2011). Similar to GPP results, a few precipitation events between September and October influenced the model and negative peaks are observed between the months June and September (2011). All approaches reproduce both phases of amplitude (positive and negative) as observed NEE.

In the analysis of NEE bias and correlation, all approaches had a reasonable (good) correlation with observed NEE data. CART ( $r^2: 0.704$ ), UNCALIBRATED ( $r^2: 0.66$ ), K-MEANS ( $r^2: 0.71$ ) and MLR ( $r^2: 0.72$ ). Figure 5b shows that the monthly totals of NEE for CART, K-MEANS and MLR reached negative values in the months of March until

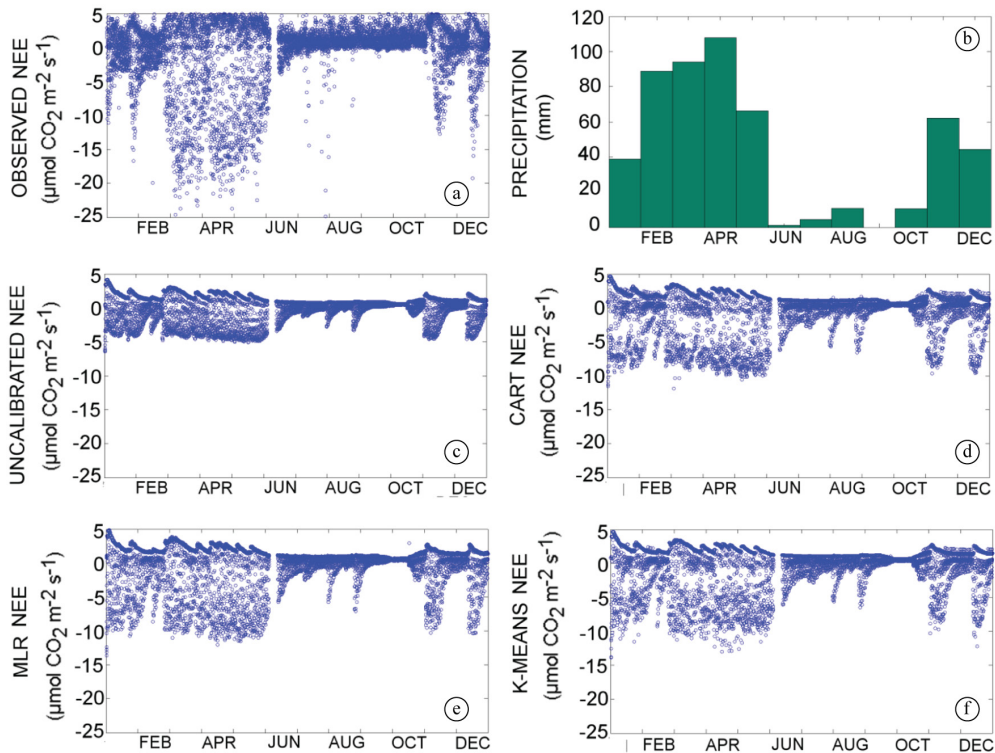


**Figure 6.** Data from 2011 - resolution of 1 hour: (a) observed NEE; (b) PRECIPITATION; (c) UNCALIBRATED NEE; (d) CART NEE; (e) MLR NEE; (f) K-MEANS NEE

May when observed data were negative since January until May. The extreme negative values for approaches CART, K-MEANS and MLR were in May:  $-695$ ,  $-720$ ,  $-844 \mu\text{mol CO}_2 \text{ m}^{-2} \text{ s}^{-1}$ , respectively. UNCALIBRATED approach was negative only in May ( $-136 \mu\text{mol CO}_2 \text{ m}^{-2} \text{ s}^{-1}$ ). Observed data had negative peak in April ( $\sim 2000 \mu\text{mol m}^{-2} \text{ s}^{-1}$ ) and in May reached  $\sim 1270 \mu\text{mol CO}_2 \text{ m}^{-2} \text{ s}^{-1}$ . In the analysis of correlation of NEE monthly totals, UNCALIBRATED approach had low correlation and CART, K-MEANS and MLR had good correlation with observed GPP data: CART ( $r^2: 0.73$ ), UNCALIBRATED ( $r^2: 0.27$ ), K-MEANS ( $r^2: 0.77$ ) and MLR ( $r^2: 0.82$ ).

#### 4. Conclusion

We showed that field measurements of ecophysiological data can contribute to the calibration of model parameters. We used data mining techniques to cope with a reduced data sample. Thus, we proposed a discretized  $V_{c_{\max}}$  value, inferred through data mining according to environmental conditions (dry or wet). After calibration of GPP, the results reached 72% of observed total GPP. CART and K-MEANS approaches had good agreement when the majority of classification cases were using node (74.96%) and group (70.92%) that had nearest mean values of  $V_{c_{\max}}$  ( $94.7 \mu\text{mol m}^{-2} \text{ s}^{-1}$  and  $92.58 \mu\text{mol m}^{-2} \text{ s}^{-1}$ , respectively). Also both algorithms (CART and K-MEANS) had few cases with high  $V_{c_{\max}}$  (greater than  $154 \mu\text{mol m}^{-2} \text{ s}^{-1}$ ) with 3.4 and 0.1% of total cases, respectively. To our knowledge, this is the first work in Brazil that uses ecophysiological data collected at semiarid environment for calibration of a DGVM. This work represents a significant contribution as a database for the *Caatinga* biome. We believe that it will be necessary to expand this database with future works. This task will enable the refinement of the calibration of DGVMs/Earth system models, since GPP could be affected directly by changes in atmospheric  $\text{CO}_2$ .

#### Acknowledgments

The authors acknowledge to Dra. Luciana Sandra Bastos de Souza (Academic Unit of Serra Talhada – UAST – Federal Rural University of Pernambuco – UFRPE), Gilson Denys (EMBRAPA) and Joemerson Ferreira Damaceno (EMBRAPA) for support in the campaigns.

L.F.C. Rezende and B. C. Arenque-Musa are grateful to Conselho Nacional de Desenvolvimento Científico e Tecnológico (CNPq) for its support under the processes 142038/2011-3 and 142308/2010-2, respectively. This work has support from Project: Impactos de mudanças climáticas sobre a cobertura e uso da terra em pernambuco: geração e disponibilização de informações para o subsídio a políticas públicas – FAPESP, Process num. 2009/52468-0 and Caatinga-FLUX: Monitoramento dos fluxos de energia,  $\text{CO}_2$  e vapor d'água e da fenologia em área de caatinga – CNPq, Process num. 483223/2011.

#### References

- BEER, C., CIAIS, P., REICHSTEIN, M., BALDOCCHI, D., LAW, B.E., PAPALE, D., SOUSSANA, J.-F., AMMANN, C., BUCHMANN, N., FRANK, D., GIANELLE, D., JANSSENS, I.A., KNOHL, A., KÖSTNER, B., MOORS, E., ROUPSARD, O., VERBEECK, H., VESALA, T., WILLIAMS, C.A. and WOHLFAHRT, G., 2009. Temporal and among-site variability of inherent water use efficiency at the ecosystem level. *Global Biogeochemical Cycles*, vol. 23, no. 2, pp. 1-13. <http://dx.doi.org/10.1029/2008GB003233>.
- BONAN, G.B., OLESON, K.W., FISHER, R.A., LASSLOP, G. and REICHSTEIN, M., 2012. Reconciling leaf physiological traits and canopy flux data: Use of the TRY and FLUXNET databases in the Community Land Model version 4. *Journal of Geophysical Research*, vol. 117, no. G02, pp. 1-19. <http://dx.doi.org/10.1029/2011JG001913>.
- BRASIL. Ministério do Meio Ambiente – MMA, 2007. *PROBIO: Projeto de Conservação e Utilização Sustentável da Diversidade Biológica Brasileira. Subprojeto: Levantamento da Cobertura Vegetal e do Uso do Solo do Bioma Caatinga*. Brasília: MMA. Relatório Final.
- BRASIL. Ministério do Meio Ambiente – MMA, 2010. *Uso sustentável e conservação dos recursos florestais da CAATINGA*. Brasília: Serviço Florestal Brasileiro.
- BRASIL. Ministério do Meio Ambiente – MMA, 2014 [viewed 16 June 2014]. *Caatinga* [online]. Brasília: MMA. Available from: <http://www.mma.gov.br/biomas/caatinga>
- BREIMAN, L., FRIEDMAN, J.H., OLSHEN, R.A. and STONE, C.J., 1984. *Classification and regression trees*. Belmont: Wadsworth Int. Group. 358 p.
- CUNHA, A.P.M.A., ALVALÁ, R.C.S., SAMPAIO, G., SHIMIZU, M.H. and COSTA, M.H., 2013. Calibration and Validation of the Integrated Biosphere Simulator (IBIS) for a Brazilian Semiarid Region. *Journal of Applied Meteorology and Climatology*, vol. 52, no. 12. <http://dx.doi.org/10.1175/JAMC-D-12-0190.1>
- DIETZE, M.C., 2014. Gaps in knowledge and data driving uncertainty in models of photosynthesis. *Photosynthesis Research*, vol. 119, no. 1-2, pp. 3-14. <http://dx.doi.org/10.1007/s11120-013-9836-z>. PMID:23645396.
- DRUMMOND, M.A., KILL, L.H.P., NASCIMENTO, C.E.S., 2002. Inventário e Sociabilidade de Espécies Arbóreas e Arbustivas da Caatinga na Região de Petrolina, PE. *Brasil Florestal*, vol. 21, no. 74, pp. 37-43.
- FARQUHAR, G.D. and VON CAEMMERER, S., 1982. Modelling of photosynthetic responses to environmental conditions. In: O.L. LANGE, P.S. NOBEL, C.B. OSMOND and H. ZIEGLER, eds. *Physiological plant ecology II*. Heidelberg: Springer-Verlag, pp. 550-587. Encyclopedia of Plant Physiology new series, vol. 12B.
- FARQUHAR, G.D., VON CAEMMERER, S. and BERRY, J.A., 1980. A biochemical model of photosynthetic  $\text{CO}_2$  assimilation in leaves of C3 species. *Planta*, vol. 149, no. 1, pp. 78-90. <http://dx.doi.org/10.1007/BF00386231>. PMID:24306196.
- FARQUHAR, G.D., SHARKEY, T., 1982. Stomatal conductance and photosynthesis. *Annals Review of Plant Physiology*. vol. 33, pp. 317-345.
- FOLEY, J.A., PRENTICE, I.C., RAMANKUTTY, N., LEVIS, S., POLLARD, D., SITCH, S. and HAXELTINE, A., 1996. An integrated biosphere model of land surface processes,

- terrestrial carbon balance, and vegetation dynamics. *Global Biogeochemical Cycles*, vol. 10, no. 4, pp. 603-628. <http://dx.doi.org/10.1029/96GB02692>.
- HAN, J. and KAMBER, M., 2001. *Data mining concepts and techniques*. San Francisco: Academic Press. 548 p.
- HUNTINGFORD, C., ZELAZOWSKI, P., GALBRAITH, D., MERCADO, L.M., SITCH, S., FISHER, R., LOMAS, M., WALKER, A.P., JONES, C.D., BOOTH, B.B.B., MALHI, Y., HEMMING, D., KAY, G., GOOD, P., LEWIS, S.L., PHILLIPS, O.L., ATKIN, O.K., LLOYD, J., GLOOR, E., ZARAGOZA-CASTELLS, J., MEIR, P., BETTS, R., HARRIS, P.P., NOBRE, C., MARENGO, J. and COX, P.M., 2013. Simulated resilience of tropical rainforests to CO<sub>2</sub>-induced climate change. *Nature Geoscience*, vol. 6, pp. 268-273 <http://dx.doi.org/10.1038/NCEO1741>.
- KUCHARIK, C.J., FOLEY, J.A., DELIRE, C., FISHER, V.A., COE, M.T., LENTERS, J.D., YOUNG-MOLLING, C., RAMANKUTTY, N., NORMAN, J.M. and GOWER, S.T., 2000. Testing the performance of a Dynamic Global Ecosystem Model: water balance, carbon balance, and vegetation structure. *Global Biogeochemical Cycles*, vol. 14, no. 3, pp. 795-825. <http://dx.doi.org/10.1029/1999GB001138>.
- LEBAUER, D., WANG, D., RICHTER, K.T., DAVIDSON, C.C. and DIETZE, M.C., 2013. Facilitating feedbacks between field measurements and ecosystem models. *Ecological Monographs*, vol. 83, no. 2, pp. 133-154. <http://dx.doi.org/10.1890/12-0137.1>.
- LIMA, G.R.T., STEPHANY, S., DE PAULA, E.R., BATISTA, I.S., ABDU, M.A., REZENDE, L.F.C., AQUINO, M.G.S. and DUTRA, A.P.S., 2014. Correlation analysis between the occurrence of ionospheric scintillation at the magnetic equator and at the southern peak of the Equatorial Ionization Anomaly. *Space Weather*, vol. 12, no. 6, pp. 406-416. <http://dx.doi.org/10.1002/2014SW001041>.
- LONG, S.P. and BERNACCHI, C.J., 2003. Gas exchange measurements, what can they tell us about the underlying limitations of photosynthesis? Procedures and sources of error. *Journal of Experimental Botany*, vol. 54, no. 392, pp. 2393-2401. <http://dx.doi.org/10.1093/jxb/erg262>. PMID:14512377.
- LONG, S.P. and HÄLLGREN, J.E., 1993. Measurements of CO<sub>2</sub> assimilation by plants in the field and laboratory. In: D.O. HALL, J.M.O. SCURLOCK, H.R. BOLHAR-NORDENKAMPF, R.C. LEEGOOD and S.P. LONG, eds. *Photosynthesis and productivity in a changing environment: a field and laboratory manual*. London: Chapman and Hall, pp. 129-167.
- MAX PLANCK INSTITUTE FOR BIOGEOCHEMISTRY, 2014 [viewed 3 February 2014]. *Eddy covariance gap-filling & flux-partitioning tool: methods* [online]. Available from: <http://www.bgc-jena.mpg.de/~MDIwork/eddyproc/method.php>
- OYAMA, M.D. and NOBRE, C.A., 2004. Climatic consequences of a large-scale desertification in northeast Brazil: A GCM simulation study. *Journal of Climate*, vol. 17, no. 16, pp. 3203-3213. [http://dx.doi.org/10.1175/1520-0442\(2004\)017<3203:CCOALD>2.0.CO;2](http://dx.doi.org/10.1175/1520-0442(2004)017<3203:CCOALD>2.0.CO;2).
- REICHSTEIN, M., FALGE, E., BALDOCCHI, D., PAPAIE, D., AUBINET, M., BERBIGIER, P., BERNHOFER, C., BÜCHMANN, N., GILMANOV, T., GRANIER, A., GRÜNWALD, T., HAVRÁNKOVÁ, K., ILVESNIEMI, H., JANOUS, D., KNOHL, A., LAURILA, T., LOHILA, A., LOUSTAU, D., MATTEUCCI, G., MEYERS, T., MIGLIETTA, F., OURCIVAL, J.-M., PUMPANEN, J., RAMBAL, S., ROTENBERG, E., SANZ, M., TENHUNEN, J., SEUFERT, G., VACCARI, F., VESALA, T., YAKIR, D. and VALENTINI, R., 2005. On the separation of net ecosystem exchange into assimilation and ecosystem respiration: review and improved algorithm. *Global Change Biology*, vol. 11, no. 9, pp. 1424-1439.
- ROGERS, A., 2014. The use and misuse of  $V_{c,max}$  in earth system models. *Photosynthesis Research*, vol. 119, no. 1-2, pp. 15-29. <http://dx.doi.org/10.1007/s1120-013-9818-1>. PMID:23564478.
- SAMPAIO, E.V.S.B., ARAÚJO, M.S.B. and SAMPAIO, Y.S.B., 2005. Impactos ambientais da agricultura no processo de desertificação do Nordeste do Brasil. XXX Congresso Brasileiro de Ciência do Solo. *Revista de Geografia*, vol. 22, no. 1, pp. 90-112.
- SANTOS, M.G., OLIVEIRA, M.T., FIGUEIREDO, K.V., FALCÃO, H.M., ARRUDA, E.C.P., ALMEIDA-CORTEZ, J., SAMPAIO, E.V.S.B., OMETTO, J.P.H.B., MENEZES, R.S.C., OLIVEIRA, A.F.M., POMPELLI, M.F., ANTONINO, A.C.D., 2014. Caatinga, the Brazilian dry tropical forest: can it tolerate climate changes? *Theoretical and Experimental Plant Physiology*, vol. 26, no. 1, pp. 83-99. <http://dx.doi.org/10.1007/s40626-014-0008-0>.
- SCHAEFER, K., SCHWALM, C.R., WILLIAMS, C., ARAIN, M.A., BARR, A., CHEN, J.M., DAVIS, K.J., DIMITROV, D., HILTON, T.W., HOLLINGER, D.Y., HUMPHREYS, E., POULTER, B., RACZKA, B.M., RICHARDSON, A.D., SAHOO, A., THORNTON, P., VARGAS, R., VERBEECK, H., ANDERSON, R., BAKER, I., BLACK, T.A., BOLSTAD, P., CHEN, J., CURTIS, P.S., DESAI, A.R., DIETZE, M., DRAGONI, D., GOUGH, C., GRANT, R.F., GU, L., JAIN, A., KUCHARIK, C., LAW, B., LIU, S., LOKIPITIYA, E., MARGOLIS, H.A., MATAMALA, R., MCCAUGHEY, J.H., MONSON, R., MUNGER, J.W., OECHEL, W., PENG, C., PRICE, D.T., RICCIUTO, D., RILEY, W.J., ROULET, N., TIAN, H., TONITTO, C., TORN, M., WENG, E. and ZHOU, X., 2012. A model-data comparison of gross primary productivity: Results from the North American Carbon Program site synthesis. *Journal of Geophysical Research*, vol. 117, no. G3, pp. 1-15. <http://dx.doi.org/10.1029/2012JG001960>.
- SMITH, N.G. and DUKES, J.S., 2012. Plant respiration and photosynthesis in global-scale models: incorporating acclimation to temperature and CO<sub>2</sub>. *Global Change Biology*, vol. 19, no. 1, pp. 45-63. PMID:23504720.
- SUTTON, C.D., 2005. Classification and regression trees, bagging and boosting. *Handbook of Statistics*, vol. 24, pp. 203-329.
- TOURIGNY, E., 2014 [viewed 9 February 2015]. *Multi-scale fire modeling in the neotropics: coupling a land surface model to a high resolution fire spread model, considering land cover heterogeneity* [online]. São José dos Campos: Instituto Nacional de Pesquisas Espaciais, 153 p. PhD Thesis in Meteorology. Available from: <http://urlib.net/8JMKD3MGP5W34M/3GD37Q2>
- VON CAEMMERER, S. and FARQUHAR, G.D., 1981. Some relationships between the biochemistry of photosynthesis and the gas exchange of leaves. *Planta*, vol. 153, no. 4, pp. 376-387. <http://dx.doi.org/10.1007/BF00384257>. PMID:24276943.
- VON CAEMMERER, S., 2000. *Biochemical models of leaf photosynthesis*. Canberra: CSIRO Publishing. 165 p.
- WITTEN, I.H., FRANK, E. and HALL, M.A., 2011. *Data mining: practical machine learning tools and techniques*. 3rd ed. Amsterdam: Elsevier.